Sensors & Diagnostics

CRITICAL REVIEW

View Article Online
View Journal | View Issue

Cite this: *Sens. Diagn.*, 2025, **4**, 451

Recent advances in nitroreductase-activatable small molecule-based photosensitizers for precise cancer therapy

Fahui Hu,†[a] Linjun Zhang,†[b] Weiqing Qiu,†[d] Jing Wang,[c] Yonsheng Liu,*[a] Wanhe Wang *[c] and Jin-Biao Liu *[a]

Received 3rd February 2025,
Accepted 31st March 2025

DOI: 10.1039/d5sd00014a

rsc.li/sensors

Photodynamic therapy (PDT) represents an innovative and highly promising modality for tumor treatment, attracting considerable attention within the medical community. However, it still faces several challenges, including limited selectivity, inadequate tissue penetration of light, and suboptimal generation of reactive oxygen species (ROS). The utilization of probes, which are activated by nitroreductase (NTR) , an enzyme that is overexpressed in hypoxic tumor tissues, for imaging and PDT represents a compelling strategy for diagnosing and treating cancerous tumors. In this review, we summarize and discuss the current progress in NTR-responsive photosensitizers for cancer imaging and therapy. We also discuss current challenges and perspectives for NTR-activatable photosensitizers. We believe these probes offer promising modalities for precise cancer therapy.

1. Introduction

Cancer cells, due to rapid proliferation and insufficient blood oxygen supply, form hypoxic regions within tumors.[1] More importantly, accumulating evidence suggests that hypoxia contributes to increased tumor invasiveness and poor prognosis.[2] Moreover, due to the scarcity of blood vessels around hypoxic cancer cells, anticancer drugs are difficult to deeply penetrate into tumor tissue, leading to poor therapeutic efficacy.[3] The overexpression of nitroreductase (NTR) under hypoxic conditions plays a crucial role in tumor progression and angiogenesis,[4] which is also an indicator of highly invasive diseases in various hypoxic cancer cells. NTR is a flavin-containing enzyme that reduces nitroaromatic compounds to the corresponding nitrites, hydroxylamines, or amino derivatives.[5] It can aid in assessing the hypoxic status of tumors and guide tumor diagnosis, treatment, and the development of activatable drugs.[6] Furthermore, NTR has been harnessed to trigger the release of prodrugs, enhancing anticancer efficacy.[7] Therefore, the NTR-activatable strategy provides new approaches for precise cancer therapy.

Photodynamic therapy (PDT) is a promising modality for cancer treatment. As a fundamental agent in PDT, photosensitizers can convert oxygen molecules into reactive oxygen species (ROS), leading to cell death. Compared to conventional chemotherapy, PDT offers precise controllability, negligible drug resistance, and non-invasiveness.[8] Although PDT has attracted significant attention as an effective treatment modality, most photosensitizers (PSs) still face challenges,[9] such as low tumor specificity, leading to the accumulation of PSs in normal tissues and causing off-target phototoxicity.[10] Additionally, some PSs induce unintended side effects in normal tissues upon light exposure,[11] limiting the clinical translation of PDT. To achieve precise treatment, it is imperative to develop advanced photosensitizers that can be selectively activated within specific tumor microenvironments, thereby enhancing the specificity and accuracy of therapeutic interventions. Given that NTR is a well-established biomarker for the hallmark of tumor hypoxia, the integration of NTR activation with concurrent photodynamic therapy (PDT) into a single molecular entity has been proposed as a promising strategy for precise cancer treatment,[12] effectively addressing the limitations associated with traditional photosensitizers in the management of hypoxic tumors.

In recent years, numerous phototherapy probes that combine NTR-specific activation with PDT have been reported through mechanisms such as photoinduced electron

[a] *Jiangxi Province Key Laboratory of Functional Crystalline Materials Chemistry, Jiangxi University of Science and Technology, Ganzhou 341000, China. E-mail: ysliu2021@jxust.edu.cn, liujinbiao@jxust.edu.cn*
[b] *Institute of Carbon Neutral New Energy, YuZhang Normal University, Nanchang 330031, China*
[c] *Institute of Medical Research, Northwestern Polytechnical University, Xian 710072, China. E-mail: whwang0206@nwpu.edu.cn*
[d] *Department of Neurology, Laizhou People's Hospital of Shangdong, Laizhou 261400, China*
† These authors are equally contributed.

transfer (PET),[13] intramolecular charge transfer (ICT),[14] and aggregation-induced emission (AIE),[15] providing dynamic information about cellular hypoxia, which are suitable for tumor diagnosis, and therapeutic evaluation. Although some good reviews have been reported for activatable PDT,[9,12,16,17] it still lacks a specific review on NTR-activatable small molecule-based photosensitizers for precise cancer therapy. This paper presents the advances in NTR-responsive PDT, which classifies and summarizes NTR-activatable photosensitizers according to three fundamental types of fluorescent mechanisms: PET, ICT and AIE. We also discuss current challenges and perspectives for this type of photosensitizers.

2. Mechanism of PDT

Since the discovery of phototoxicity in some dyes in the early 20th century, PDT has steadily advanced with the continuous development of photochemistry and photophysics.[18] PDT induces apoptosis and vascular closure, ultimately removing lesions, by utilizing photosensitizers administered systemically and generating localized ROS upon laser irradiation of the affected area.[19,20] Traditionally, PDT is classified into type I PDT and type II PDT (Fig. 1), depending on the different photochemical processes involved.[21] The photosensitizer absorbs a photon with an appropriate wavelength, transitioning from its ground state (S_0) to the first singlet excited state (S_1) or the second singlet excited state (S_2). S_2 rapidly decays to S_1 through internal conversion (IC). S_1 is also unstable, with a lifetime on the nanosecond scale, thus deactivating through either fluorescence emission or heat generation during the IC process. At the same time, S_1 may undergo intersystem crossing (ISC), forming a more stable triplet excited state (T_1).[22] T_1 exhibits a longer lifetime (microseconds), and it directly reacts with intracellular biological substrates, generating free radicals through hydrogen or electron transfer processes. These free radicals may further react with O_2 and water to produce ROS, including hydroxyl radicals (·OH) and superoxide anions ($O_2^{\bullet-}$). However, in type II PDT, T_1 participates in type II photochemical reactions, transferring energy to convert ground-state O_2 into highly cytotoxic singlet oxygen ($^1O_2$).[23] Thus, the type II process primarily occurs under normoxic conditions but is limited under hypoxic conditions, while the type I process can occur in both normoxic and hypoxic microenvironments.

3. NTR-activatable small molecule-based photosensitizers based on the PET mechanism for PDT

PET is an excited-state electron transfer process, where an excited-state electron transfers to a ground-state molecules.[24] The classic structure of a PET probe consists of a fluorophore conjugated to the recognition receptor *via* a spacer group. The intramolecular electron transfer between the recognition receptor and the fluorophore leads to fluorescence quenching (Fig. 2c).[25] When the target binds to the recognition receptor, the PET process is inhibited, thus the probe's fluorescence is restored. Typically, PET includes two processes, a-PET and d-PET,[26] depending on the direction of electron transfer (Fig. 2). (1) In the a-PET process, electron transfer occurs from the receptor to the fluorophore, as the highest occupied molecular orbital (HOMO) of the receptor is at a higher energy level than that of the fluorophore (Fig. 2a). (2) In contrast, during d-PET, the photoexcited electron of the fluorophore transfers to the lowest unoccupied molecular orbital (LUMO) of the receptor, leading to fluorescence quenching (Fig. 2b).

In addition to being an important strategy for designing "on–off" or "off–on" fluorescence probes, PET can also be used to regulate the generation of $^1O_2$ in photodynamic therapy. It is well known that the quantum yield of $^1O_2$ is directly related to the efficiency of ISC (generally, high ISC efficiency results in a high $^1O_2$ quantum yield), but PET and

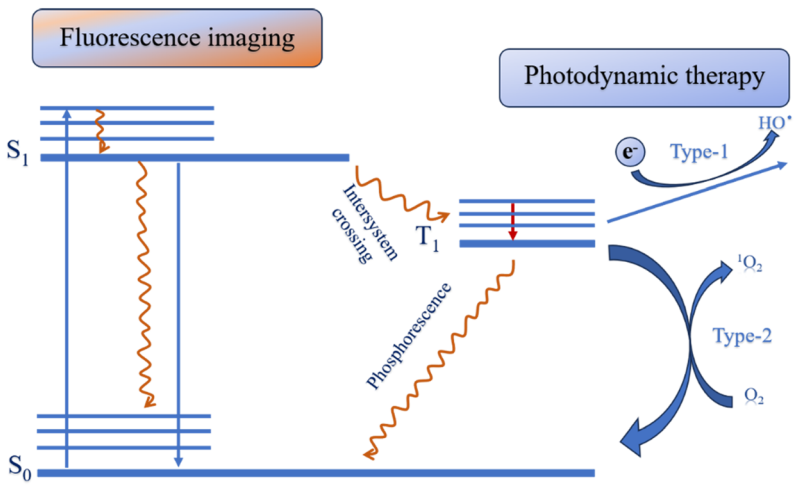

Fig. 1 The mechanism diagram of PDT.

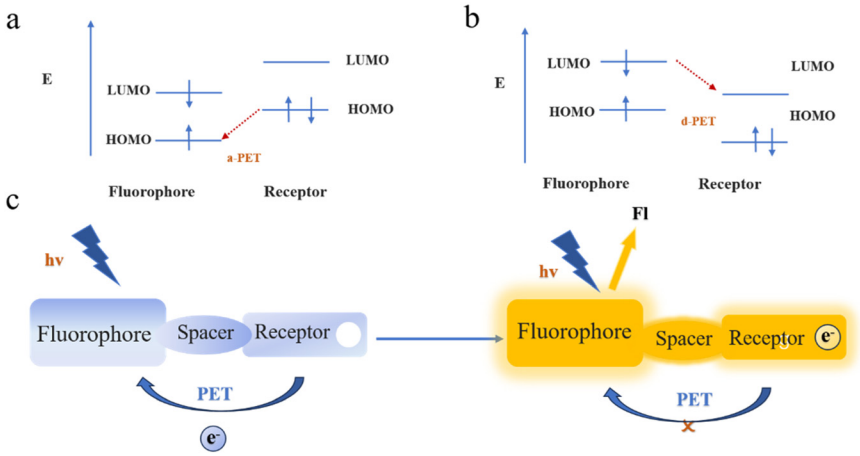

Fig. 2 Schematic illustration of the mechanism based on PET.

ISC are competitive with each other in the process of deactivation of excited states. Therefore, inhibiting PET can significantly enhance the efficiency of ISC, thereby increasing the $^1O_2$ quantum yield. Thus, the generation of $^1O_2$ can be controlled by modulating the PET process.[27] Based on this observation, PET has also become as a common strategy for NTR-activatable small molecule-based photosensitizers.

Common fluorescence-quenching groups in photosensitizers typically contain a nitro group. The LUMO of the nitro group is at a lower energy level, so the triggering mechanism of such NTR probes is often d-PET.[28] When the nitro-recognizing group is reduced to an amino group by NTR, the nitro-induced electron transfer process is quenched, thereby activating fluorescence. In the past two years, the application of NTR-activatable small molecule-based photosensitizers based on the PET mechanism has significantly developed. Here, this section discusses strategies for imaging and therapy of hypoxic tumors using NTR-activatable small molecule-based photosensitizers based on PET (Table 1).

The development of novel phototherapeutic probes with near-infrared (NIR) fluorescence and photosensitizing capabilities can effectively improve the efficiency of PDT. These probes are more suitable for *in vivo* imaging and therapy due to their advantages, including deeper tissue penetration, reduced photodamage, and lower background fluorescence interference. Li *et al.* reported a highly sensitive NIR phototheranostic probe (HCN)[29] for detecting the hypoxic state of tumors and inhibiting tumor proliferation through the PDT process. HCN is the first NTR-responsive fluorescent probe capable of imaging tumors as small as 6 mm^3. Similarly, Zheng *et al.* developed a novel NIR photosensitizer-CYNT-1 (Fig. 3a),[30] which demonstrated confocal fluorescence imaging with a depth of up to 160 μm and exhibited efficient PDT effects in a HeLa cell 3D spheroid model.

Achieving precise control of tumor hypoxia imaging while performing PDT has been a significant challenge. Chen *et al.* designed a liposome-based theranostic nanoprobe (DiBDP), which features an orthogonally linked dimeric BODIPY (Ab-DiBDP NPs)[31] structure and incorporates a nitro group. Through the synergistic interaction between the Cy7-labeled anti-HIF-1α antibody and the NTR-activated DiBDP, this approach significantly enhances the accuracy of tumor hypoxia imaging by simultaneously detecting NTR and HIF-1α.

Table 1 Summary of NTR-activatable small molecule photosensitizers

Compound	Emission	Stimulus	Photosensitizer	$^1O_2$ quantum yields	Therapeutic modalities	Tumors	IC_{50} (μM)	Ref.
HCN	758 nm	660 nm	Hemicyanine	—	PDT	A549	—	29
CYNT-1	635 nm	660 nm	Cy7	—	PDT	HeLa	—	30
Ab-DiBDP NPs	650 nm	520 nm	BODIPY	52%	PDT	HeLa	—	31
Compound 2	635 nm	590 nm	Fluorescein	—	PDT	HeLa	5.91	32
CLN	758 nm	660 nm	Cyanine-based derivative	1.0.6%	PDT	4T1	7.4	33
Cy7-X-NO_2	803 nm	785 nm	Heptamethine aminocyanine dye	8.5%	PDT/PA/PTT	C4-2	—	34
Icy-NBF	837 nm	808 nm	Iodinated heptamethine cyanine	16.4%	PDT/PTT	HeLa	—	35
CyNP	790 nm	760 nm	IR780	4.7%	PDT/PTT	HeLa	0.60	36
BPN 2	720 nm	680 nm	Benzophenothiazine	—	PDT/PA	EMT6	—	37
Eos-NO_2	532 nm	532 nm	Eosin Y (Eos)	—	PDT/radical-induced damage	SCC	—	38
NFh-NTR	745 nm	808 nm	Hemicyanine	5.89%	PDT	A549	—	39

Note: IC_{50}: inhibitory concentration 50%.

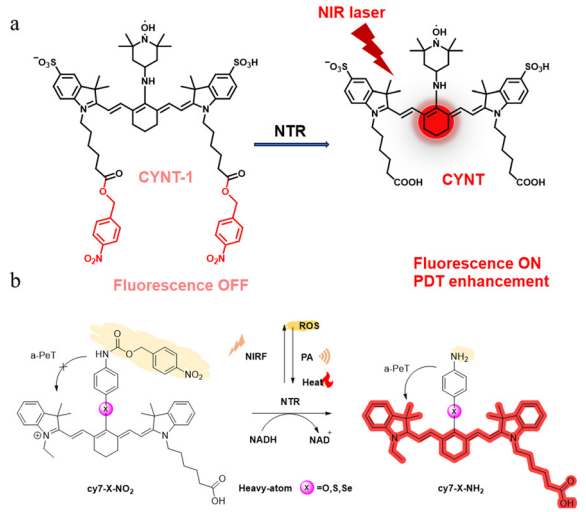

Fig. 3 (a) The structure of CYNT-1 and its deduced enzyme-catalyzed mechanism activated with NTR. Reproduced with permission.[38] Copyright 2020 Royal Society of Chemistry. (b) Structures of Cy7-X-NH_2 and Cy7-X-NO_2 (X = O, S, Se), and response mechanism of Cy7-X-NO_2 toward NTR. Reproduced with permission.[40] Copyright 2024 Elsevier.

The short lifespan of ROS (approximately 3.5 μs) and their limited diffusion distance (around 2 μm) restrict their phototoxicity at the localized sites of PSs. The efficacy of PDT largely depends on the intracellular localization of the photosensitizer molecules. Liu *et al.* developed an NTR-activated, lysosome-targeting smart PDT photosensitizer (compound **2**)[32] using a low-toxicity thermally activated delayed fluorescence (TADF) fluorophore derivative. In addition to its NTR-activated theranostic properties, compound **2** offers several other advantages, including two-photon excitation, a large Stokes shift, short response time, and high specificity and sensitivity. Importantly, the strategy of targeting mildly hypoxic cells at the tumor margin addresses the "fatal weakness" of traditional PDT. In addition, Ding *et al.* designed and synthesized a novel NTR-activated cyanine-based PS (CLN),[33] which is also capable of effectively targeting the lysosome. Moreover, the maximum absorption wavelength of CLN lies in the red light region.

The mitochondrion, regarded as the control center of cell apoptosis and the cell's energy factory, is essential for maintaining normal cell function and health. More importantly, mitochondria are highly sensitive to heat and ROS, making them an ideal target for organelle-specific phototherapy that triggers apoptosis. Based on the synergistic treatment of PDT and photothermal therapy (PTT), Wu *et al.* designed a mitochondrial NTR-activated photoacoustic (PA) probe (Cy7-X-NO_2).[34] The probe's inherent ability to target mitochondria facilitated its accumulation in tumors, enabling highly effective antitumor effects through PDT. The overexpression of NTR in solid tumors reduces the *p*-nitrobenzyl chloroformate group, triggering the release of Cy7-X-NO_2 *via* rearrangement and elimination mechanisms (Fig. 3b). This process enhances the PA signal output, allowing *in vivo* visualization of the tumor region and significantly inhibiting tumor growth through the combined application of PDT and PTT.

The combined application of PTT and PDT has emerged as a promising strategy for tumor treatment. However, designing photosensitizers with high photothermal efficiency and excellent photodynamic performance remains a challenging task. Zhao *et al.* proposed a molecular design (Icy-NBF)[35] based on the regulation of oxygen content to control the excited-state deactivation process. Under the action of NTR overexpressed in hypoxic cancer cells, Icy-NBF is reduced and converted into a molecule (Icy-NH_2) with the same backbone. The excited-state deactivation pathway of Icy-NBF is altered after the NTR-mediated reduction. As the oxygen concentration in cancer cells decreases, the photosensitizer generated from Icy-NBF transitions from $^1O_2$ to heat, thereby enabling PTT. In contrast, Zhao *et al.* proposed a molecular design (CyNP),[36] where in the tumor's normoxic regions, the excited-state deactivation pathway of CyNP primarily involves the conversion of photon energy into heat. However, in the tumor's hypoxic regions, CyNP is reduced to CyNH by nitroreductase, and the deactivation pathways mainly include radiative transitions, energy transfer between CyNP and oxygen, and the conversion of photon energy into heat, thereby transforming PDT into a synergistic PDT-PTT.

Unlike O_2-dependent type II PDT, O_2-dependent type I PDT reduces the demand for oxygen by avoiding direct and rapid consumption of oxygen, showing great potential in overcoming hypoxic cancer. Activatable type I photosensitizers provide an effective approach to address the shortcomings and inaccuracy of PDT in hypoxic tumors. Zeng *et al.* designed a novel hypoxia-responsive Pro-PS (BPN 2)[37] by modifying the 2-methoxy-4-nitrophenyl dye, which enables background-independent fluorescence/photoacoustic bimodal tumor imaging upon NTR activation. After activation, BPN 2 can simultaneously generate oxygen-independent photoacoustic cavitation effects and type I photodynamic processes under single-pulse laser irradiation.

Furthermore, to avoiding directly and rapidly consuming activated-type photosensitizers of type I, Xue *et al.* developed a new NTR-activated photodynamic mechanism using eosin Y (Eos-NO_2),[38] which can generate free radicals (·Eos) under hypoxic conditions (5% oxygen, V_{O_2}/V_{N_2}) for the effective treatment of hypoxic tumors. Furthermore, it is also capable of efficiently generating ROS under normoxic conditions (20% oxygen, V_{O_2}/V_{N_2}) to perform PDT.

Notably, recent advancements in PET-based designs have expanded into heavy-atom-free systems for improved biosafety. A groundbreaking study by Liu *et al.* (2024) developed NFh-NTR, a nitrobenzyl-modified upconversion photosensitizer that achieves tumor-specific activation through NTR-mediated PET process modulation.[39] This system cleverly inhibits singlet oxygen generation *via* suppressed charge separation (CS) states until enzymatic activation, resolving the "always-on" toxicity dilemma prevalent in conventional photosensitizers. Its unique

frequency upconversion luminescence (FUCL) mechanism enables deep-tissue 808 nm excitation while maintaining hypoxia-specific activation profiles, representing a significant leap from earlier visible-light PET probes like Kiyose's fluorescein derivatives. This work exemplifies how modern PET systems integrate multiple photophysical principles (FUCL + PET) to enhance therapeutic precision.

4. NTR-activatable small molecule-based photosensitizers based on the ICT mechanism for PDT

The ICT property refers to the transfer of a charge from one part of a molecule to another through a conjugated path (Fig. 4), typically by introducing an electron donor into an electron acceptor part.[41] This mechanism is another widely used approach for fluorescent probes. The charge transfer can occur over long distances and is associated with significant changes in the dipole moment, making it particularly sensitive to the microenvironment of the fluorophore.[42]

Consequently, cations or anions that closely interact with the donor or acceptor parts alter the photophysical properties of the fluorophore. This process also induces changes in the absorption and emission spectra, manifested as red or blue shifts, known as Stokes shifts.[43] Therefore, ICT probes are typically designed as "turn-on" types to enhance sensitivity.

Notably, ICT strongly influences fluorescence and $^1O_2$ generation by competing with other deactivation processes, such as ISC and PET. Peng *et al.* designed a NIR photosensitizer by incorporating selenium into heptamethine cyanine.[44] The ICT between the selenium atom and the polymethine chain reduced the energy gap (ΔE_{ST}) while enhancing spin-orbit coupling (SOC), effectively inducing ultra-efficient $^1O_2$ generation. Zimcik *et al.* investigated the ICT process in a series of magnesium, metal-free, and zinc complexes of unsymmetrical tetrapyrazinoporphyrazines and tribenzopyrazinoporphyrazines.[40] These complexes, which contain two dialkylamino substituents (donors), undergo ICT that deactivates the excited states leading to a significant decrease in fluorescence and $^1O_2$ quantum yields. Many small molecule fluorescent probes based on the ICT mechanism have been designed for detection of biomolecules;[45,46] specifically, it is also applied for the development of NTR-activatable photosensitizers (Table 2).

Xu *et al.* synthesized a hypoxia-activated NIR photosensitizer (ICy-N),[47] which exhibits NIR emission (λ_{em} = 716 nm) and mitochondrial targeting ability. Under 660 nm irradiation, it demonstrates efficient $^1O_2$ generation, effectively inducing cell apoptosis (IC_{50} = 0.63 μM). In addition to targeting the mitochondria, Zhang *et al.* developed an ICT PS with inherent endoplasmic reticulum (ER) targeting ability, named ^{ER}PSIm.[48] ^{ER}PSIm exhibits type I PDT effects and enhances the therapeutic efficacy of PDT on tumor cells under both normoxic and hypoxic conditions.

Wei *et al.* reported a dual-lock activation phototherapeutic diagnostic probe (DHP)[49] that can activate near-infrared fluorescence (NIRF) signals in tumors and trigger PDT in response to tumor edge biomarkers (Fig. 5). Upon detection of hypoxic biomarkers in the tumor core, the probe switches from PDT to PTT. This PDT-PTT auto-regulated probe effectively eliminates tumors by generating cytotoxic $^1O_2$ at the tumor edge and inducing hyperthermia at the tumor core. Numerous probes and photosensitizers based on the synergistic PTT-PDT strategy have been developed.[53,54] In addition, probes combining PDT with other therapeutic strategies have also attracted considerable interest. Zhang *et al.* designed a novel PDT-chemotherapy nanodrug (Cy-NTR-CB).[50] Unlike traditional HAP (tumor-activated prodrugs), Cy-NTR-CB features a nitrobenzyl recognition site positioned in the middle of the linker chain. Under hypoxic conditions, Cy-NTR-CB is reduced by NTR to an aromatic amine, triggering electron rearrangement and a domino-like decomposition reaction, ultimately releasing the activated chemotherapy drug.

For light-excited probes and photosensitizers, background signals from tissue autofluorescence can interfere with diagnostic sensitivity. In contrast, chemiluminescence therapeutic diagnostics do not require real-time light excitation, thus overcoming the issue of tissue autofluorescence. Huang *et al.* reported a NIR chemiluminescent compound ($HEDP_N$),[51] with specific binding affinity for human serum albumin (HSA), which forms a chemiluminescent compound–protein complex. The binding of the protein complex enhances the chemiluminescence signal by more than 10-fold by inhibiting

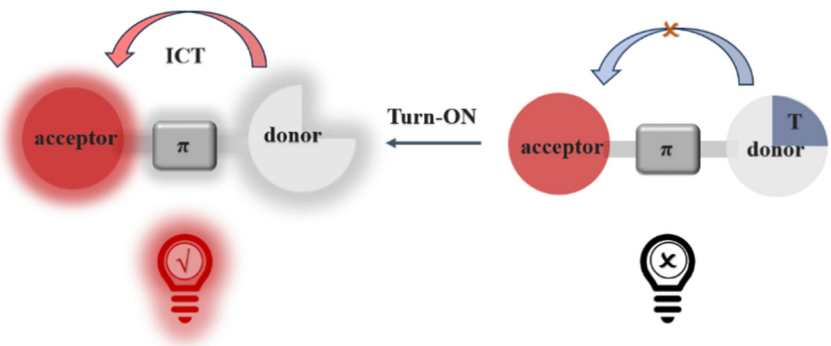

Fig. 4 Schematic illustration of the mechanism based on ICT.

Table 2 Summary of NTR-activatable small molecule photosensitizers

Compound	Emission	Stimulus	Photosensitizer	$^1O_2$ quantum yields	Therapeutic modalities	Tumors	IC_{50} (μM)	Ref.
ICy-N	710 nm	660 nm	Hemicyanine dye	0.72%	PDT/PTT	4T1	0.63	47
^{ER}PSIm	660 nm	490–700 nm	—	—	PDT	4T1	—	48
DHP	725 nm	680 nm	Hemicyanine	1.18%	PDT/PTT	HeLa	—	49
Cy-NTR-CB	720 nm	660 nm	Cyanine dyes	—	PDT/chemotherapy	4T1	<0.60	50
$HEDP_N$	700 nm	White light	*N*-Ethylrhodanine moiety	—	PDT/PTT	4T1	—	51
CyNT-F	720 nm	655 nm	Hemicyanine azide-derivative	1%	PDT	4T1	—	52

Note: IC_{50}: inhibitory concentration 50%.

non-radiative decay and participating in electron transfer reactions, thereby converting type-II PDT into type-I PDT.

Another challenge in targeted cancer therapy is the extensive accumulation and prolonged retention of photosensitizers at the tumor site. Due to the rapid metabolism of tumor tissues, photosensitizers can easily exit the target cells and enter surrounding normal cells, leading to therapeutic side effects. Zhu *et al.* proposed a stimulus-triggered self-immobilization strategy (CyNT-F)[52] that effectively reduces the diffusion of photosensitizers by enhancing their binding affinity to cellular proteins. They introduced a difluoromethylated quinone precursor, which, upon enzymatic stimulation, forms an electrophilic quinone that covalently binds to nucleophilic groups on nearby proteins, thereby activating fluorescence and PDT. Because macromolecular proteins have limited permeability across cell membranes, the activated photosensitizer can accumulate and remain in the tumor for an extended period, effectively inhibiting tumor growth.

5. NTR-activatable small molecule-based photosensitizers based on the AIE mechanism for PDT

The aggregation-caused quenching (ACQ) phenomenon inherent in traditional PSs weakens their fluorescence, thereby limiting their therapeutic efficacy. To overcome ACQ, Tang and his colleagues first proposed the concept of AIE in 2001.[55] AIE describes a photophysical phenomenon in which certain non-emissive molecules in solution are induced to emit bright fluorescence upon aggregation (Fig. 6) In most cases, restricted intramolecular motion (RIM) has been identified as the primary cause of AIE.[56] In the molecular state, the energy of AIE molecules can be dissipated through free intramolecular motions, including rotation and vibration. Upon aggregation, intermolecular interactions can block these free movements, thus limiting the associated non-radiative decay pathways. As a result, the absorbed excitation energy is redirected to other pathways, namely fluorescence emission and ISC to generate ROS.[57] Incorporating AIE characteristics into photosensitizers represents a strategic advancement, amplifying their fluorescence in the aggregated state and enhancing their biomedical potential.

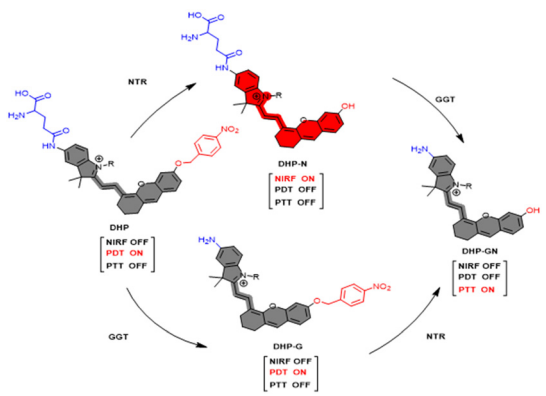

Fig. 5 Scheme describing the molecular mechanism of DHP for real-time imaging of tumor and auto-regulated PDT-PTT in the presence of GGT and NTR. Reproduced with permission.[50] Copyright 2022 German Chemical Society.

Additionally, AIEgens exhibit notable photophysical properties such as large Stokes shifts, excellent photostability, and long retention times in live samples.[58–60] Prior to the development of the AIE-PDT system, critical foundational works focused on highly sensitive detection of NTR. The TPE-HY probe developed by Xu *et al.* first integrated the AIE properties of tetraphenylethylene (TPE) with NTR responsiveness, providing significant inspiration for the design rationale of subsequent therapeutic probes.[61] This probe achieves fluorescence quenching through the reduction of nitro ($-NO_2$) to amino ($-NH_2$) groups, triggering intramolecular charge transfer inhibition, leading to signal equilibration within 5 minutes. This "reverse activation" mechanism breaks through the enhancement mode of conventional AIE probes. Although not directly applied to PDT, its innovation established a molecular template for the targeted design of subsequent therapeutic AIE-PDT probes.

The discovery and development of AIE fluorophores have opened new opportunities for PDT. Here, this section discusses strategies for imaging and therapy of hypoxic tumors using AIE-based NTR-activatable small molecule probes and photosensitizers (Table 3).

For example, Wang *et al.* developed an NTR-triggered lysosome-targeting probe based on a TPE core M-TPE-P (Fig. 7).[62] This probe specifically detects NTR in the acidic lysosomal microenvironment (pH 4.5–5), exhibiting high selectivity and sensitivity, with a catalytic efficiency of K_{cat}/K_m

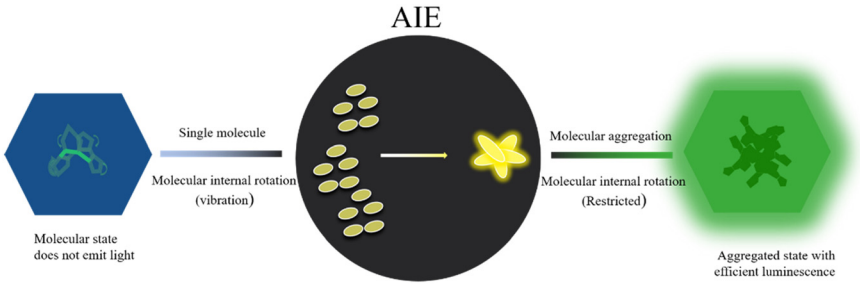

Fig. 6 Schematic illustration of the AIE mechanism.

Table 3 Summary of NTR-activatable small molecule photosensitizers

Compound	Emission	Stimulus	Photosensitizer	$^1O_2$ quantum yields	Therapeutic modalities	Tumors	IC_{50} (μM)	Ref.
M-TPE-P	618 nm	808 nm	Tetraphenylethene	—	PDT	4T1 cells	—	62
T-TPE-NO_2	626 nm	365 nm	Tetraphenylethene	—	PDT	HepG2	—	63
TTVP	708 nm	White light	Nitrobenzoic acid	80.16%	PDT	HeLa	—	64
Biotin-TTVBA	535 nm	White light	Nitrobenzoic acid	16%	PDT	HeLa	2.5	65
NTPy	678 nm	488 nm	Triphenylamine derivatives	—	PDT	HeLa	—	66

Note: IC_{50}: inhibitory concentration 50%.

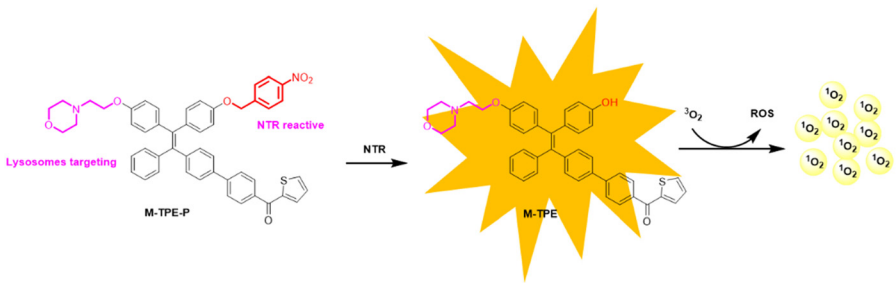

Fig. 7 Schematic representation of the NTR-responsive fluorescence turn-on photosensitizer for lysosome imaging and PDT. Reproduced with permission.[61] Copyright 2024 Elsevier.

(turnover number/Michaelis constant) value of 2.18×10^4 M^{-1} s^{-1} and a detection limit as low as 53.6 ng mL^{-1}. More importantly, the narrow ΔE_{ST} and efficient ROS generation make this probe a promising PDT photosensitizer. Similarly, Huang *et al.* developed a novel mitochondria-targeted fluorescence probe based on a TPE core, T-TPE-NO_2, which exhibits typical AIE characteristics.[63] The probe exhibits typical AIE characteristics, undergoing aggregation in the presence of NTR, which leads to an increase in fluorescence signal. The probe displays high selectivity and sensitivity to NTR across a wide pH range, enabling effective detection and imaging of tumor hypoxia. Additionally, upon light irradiation, T-TPE-NO_2 significantly produces ROS to induce mitochondrial damage, and triggers apoptosis, demonstrating strong antitumor activity. At a concentration of 20 μM of T-TPE-NO_2, the cell viability of HepG2 cells decreased to about 30%. This probe represents significant progress in the development of multifunctional probes for cancer therapy, offering dual diagnostic and therapeutic capabilities.

Tang *et al.* first reported a water-soluble near-infrared emitting AIE photosensitizer (TTVP).[64] The probe hardly emits fluorescence in aqueous solution due to its good water solubility, which results from the cationic quaternary ammonium and pyridinium ligands. These cationic ligands enable TTVP to bind to negatively charged cell membranes, especially cancer cell membranes, which have a more negatively charged surface. When interacting with the cell membrane, the hydrophilic part of the probe cannot quickly pass through the membrane due to the hydrophobic nature of the membrane's interior, while the hydrophobic emitting segment embeds into the hydrophobic region of the membrane bilayers. By utilizing its AIE characteristics, rapid no-wash imaging of the cell membrane can be achieved within seconds. In addition, TTVP with a D–A structure has a small ΔE_{ST} (0.47 eV), making it an efficient NIR photosensitizer with a high $^1O_2$ quantum yield of 80.16%, which nearly completely eradicates cancer cells under white light irradiation even at a low concentration of 1 μM, highlighting its high efficiency for PDT applications. The

combination of light-controlled cancer cell killing and fluorescence emission in the NIR region makes TTVP an attractive candidate for imaging-guided PDT.

Most traditional photosensitizers lack cancer cell targeting ability, leading to reduced PDT efficacy and potential side effects. Therefore, targeted PDT has become a key focus for researchers. Wang *et al.* also developed a fluorescent tumor-targeting AIE photosensitizer based on nitroaromatic groups (Biotin-TTVBA).[65] By incorporating a tumor-targeting biotin group, this probe significantly enhanced selective uptake by tumor cells, thereby improving its anticancer activity and reducing the IC_{50} value from >40 μM to 2.5 μM.

Recently, Huang's group designed a novel AIEgen probe (NTPy),[66] which utilizes 4-nitrobenzene as the NTR recognition group. NTPy can detect the tumor hypoxic microenvironment through a fluorescence "turn-off" mechanism, showing a significant fluorescence emission at 678 nm. The difference in fluorescence intensity between NTPy and TPy allows for the intuitive detection of hypoxia in tumors. The degradation product TPy exhibits good biocompatibility and low PDT activity. Therefore, by controlling the dosage of NTPy and the PDT treatment duration, efficient PDT can be achieved with reduced side effects. This provides a new strategy to improve the biosafety of residual photosensitizers after PDT treatment without compromising therapeutic efficacy.

6. Conclusions

In summary, we reviewed the current NTR-activatable small molecule photosensitizers for precise PDT, based on three activatable mechanisms of fluorescent probes. Given the overexpression of NTR in hypoxic solid tumors, the NTR-activatable photosensitizers achieve desirable therapeutic outcomes in hypoxic tumors, and also potentially provide valuable insights into the biological functions of NTR, which are suitable for early diagnosis of cancers.

Despite significant progress in the development of NTR-activatable small molecule photosensitizers for PDT, there remain many unresolved issues and challenges. Most of these probes and photosensitizers are based on type II PDT, whose effectiveness is largely limited by the oxygen dependency. Furthermore, strategies that combine PDT with other therapeutic modalities are gaining increasing interest among researchers. Developing probes and photosensitizers that synergize with other treatments, such as sonodynamic therapy (SDT) and chemotherapy, could potentially enhance therapeutic outcomes. Moreover, most NTR-activatable photosensitizers have short excitation wavelengths, severely limiting tissue penetration depth. Therefore, the development of NTR-activatable photosensitizers excited by NIR light is essential. Moreover, multiphoton excitation and chemical excitation offer deeper tissue penetration and greater therapeutic precision for PDT, potentially opening new avenues for PDT. In addition to the aforementioned challenges, studying the *in vivo* biodistribution, long-term biocompatibility, and pharmacokinetics of NTR probes is crucial for future clinical translation. We hope this review will stimulate the interest of researchers from various disciplines to leverage the unique advantages of NTR-activatable small molecule photosensitizers, leading to the development of more specific and selective photosensitive probes, thus advancing the progress of phototherapy in precision tumor therapy.

Data availability

No primary research results, software or code have been included and no new data were generated or analysed as part of this review.

Author contributions

Methodology, J.-B. Liu and F. H. Hu; data curation, F. H. Hu; writing – original draft preparation, F. H. Hu; writing – review and editing, J.-B. Liu, W. Q. Q., W. W., L. J. Zhang, J. W. and Y. Liu; supervision, J.-B. Liu, W. W. and J. W.; project administration, W. Q. Q., J.-B. Liu and W. W.; funding acquisition, J.-B. Liu, W. W., and J. W. All authors have read and agreed to the published version of the manuscript.

Conflicts of interest

There are no conflicts to declare.

References

1 P. Vaupel and A. Mayer, *Cancer Metastasis Rev.*, 2007, **26**, 225–239.
2 C. Liao, X. Liu, C. Zhang and Q. Zhang, *Semin. Cancer Biol.*, 2023, **88**, 172–186.
3 A. L. Harris, *Nat. Rev. Cancer*, 2002, **2**, 38–47.
4 J. M. Brown and W. R. William, *Nat. Rev. Cancer*, 2004, **4**, 437–447.
5 J.-n. Liu, W. Bu and J. Shi, *Chem. Rev.*, 2017, **117**, 6160–6224.
6 C. Berne, L. Betancor, H. R. Luckarift and J. C. Spain, *Biomacromolecules*, 2006, **7**, 2631–2636.
7 H. Zhang, C. Shi, F. Han, L. Cai, H. Ma, S. Long, W. Sun, J. Du, J. Fan and X. Chen, *Biomaterials*, 2023, **302**, 122365.
8 S. Kwiatkowski, B. Knap, D. Przystupski, J. Saczko, E. Kędzierska, K. Knap-Czop, J. Kotlińska, O. Michel, K. Kotowski and J. Kulbacka, *Biomed. Pharmacother.*, 2018, **106**, 1098–1107.
9 T. C. Pham, V.-N. Nguyen, Y. Choi, S. Lee and J. Yoon, *Chem. Rev.*, 2021, **121**, 13454–13619.
10 S. Son, J. Kim, J. Kim, B. Kim, J. Lee, Y. Kim, M. Li, H. Kang and J. S. Kim, *Chem. Soc. Rev.*, 2022, **51**, 8201–8215.
11 Y. Li, G. He, L.-H. Fu, M. R. Younis, T. He, Y. Chen, J. Lin, Z. Li and P. Huang, *ACS Nano*, 2022, **16**, 17298–17312.
12 E. Nestoros, A. Sharma, E. Kim, J. S. Kim and M. Vendrell, *Nat. Rev. Chem.*, 2025, **9**, 46–60.
13 A. Xu, Y. Tang, Y. Ma, G. Xu, S. Gao, Y. Zhao and W. Lin, *Sens. Actuators B: Chem.*, 2017, **252**, 927–933.

14 J. Yuan, Y.-Q. Xu, N.-N. Zhou, R. Wang, X.-H. Qian and Y.-F. Xu, *RSC Adv.*, 2014, **4**, 56207–56210.
15 X. Tian, L. C. Murfin, L. Wu, S. E. Lewis and T. D. James, *Chem. Sci.*, 2021, **12**, 3406–3426.
16 Q. Sun, Z. Wang, B. Liu, F. He, S. Gai, P. Yang, D. Yang, C. Li and J. Lin, *Coord. Chem. Rev.*, 2022, **451**, 214267.
17 S. Zhi, M. Huang and K. Cheng, *Drug Discovery Today*, 2024, **29**, 103965.
18 M. D. Daniell and J. S. Hill, *Aust. N. Z. J. Surg.*, 1991, **61**, 340–348.
19 Y. Xia, Q. Liu, H. Zhang, X. Yang, L. He and D. Cheng, *Sens. Actuators B: Chem.*, 2024, **419**, 136382.
20 P. Agostinis, K. Berg, K. A. Cengel, T. H. Foster, A. W. Girotti, S. O. Gollnick, S. M. Hahn, M. R. Hamblin, A. Juzeniene and D. Kessel, *Ca-Cancer J. Clin.*, 2011, **61**, 250–281.
21 M. Lan, S. Zhao, W. Liu, C. S. Lee, W. Zhang and P. Wang, *Adv. Healthcare Mater.*, 2019, **8**, 1900132.
22 G. Yang, S. Hao, X. Deng, X. Song, B. Sun, W. J. Hyun, M.-D. Li and L. Dang, *Nat. Commun.*, 2024, **15**, 4674.
23 D. Chen, Q. Xu, W. Wang, J. Shao, W. Huang and X. Dong, *Small*, 2021, **17**, 2006742.
24 W. Sun, M. Li, J. Fan and X. Peng, *Acc. Chem. Res.*, 2019, **52**, 2818–2831.
25 I. Willner, E. Kaganer, E. Joselevich, H. Dürr, E. David, M. J. Günter and M. R. Johnston, *Coord. Chem. Rev.*, 1998, **171**, 261–285.
26 W. Chi, J. Chen, W. Liu, C. Wang, Q. Qi, Q. Qiao, T. M. Tan, K. Xiong, X. Liu, K. Kang, Y.-T. Chang, Z. Xu and X. Liu, *J. Am. Chem. Soc.*, 2020, **142**, 6777–6785.
27 W. Wu, X. Shao, J. Zhao and M. Wu, *Adv. Sci.*, 2017, **4**, 1700113.
28 T. MarekáKrygowski, *Chem. Soc. Rev.*, 1996, **25**, 71–75.
29 L. Li, L. Ding, X. Zhang, D. Wen, M. Zhang, W. Liu, H. Wang, B. Wang, L. Yan, L. Guo and H. Diao, *Spectrochim. Acta - A: Mol. Biomol. Spectrosc.*, 2022, **267**, 120579.
30 J. Zheng, Y. Liu, F. Song, L. Jiao, Y. Wu and X. Peng, *Chem. Commun.*, 2020, **56**, 5819–5822.
31 H. Chen, Q. Bi, Y. Yao and N. Tan, *J. Mater. Chem. B*, 2018, **6**, 4351–4359.
32 Z. Liu, F. Song, W. Shi, G. Gurzadyan, H. Yin, B. Song, R. Liang and X. Peng, *ACS Appl. Mater. Interfaces*, 2019, **11**, 15426–15435.
33 S. Ding, M. Yang, J. Lv, H. Li, G. Wei, J. Gao and Z. Yuan, *Molecules*, 2022, **27**, 3457.
34 L.-L. Wu, X. Meng, Q. Zhang, X. Han, F. Yang, Q. Wang, H.-Y. Hu and N. Xing, *Chin. Chem. Lett.*, 2024, **35**, 108663.
35 X. Zhao, S. Long, M. Li, J. Cao, Y. Li, L. Guo, W. Sun, J. Du, J. Fan and X. Peng, *J. Am. Chem. Soc.*, 2020, **142**, 1510–1517.
36 D. Shen, S. Ding, Q. Lu, Z. Chen, L. Chen, J. Lv, J. Gao and Z. Yuan, *ACS Omega*, 2024, **9**, 30685–30697.
37 Q. Zeng, X. Li, J. Li, M. Shi, Y. Yao, L. Guo, N. Zhi and T. Zhang, *Adv. Sci.*, 2024, **11**, 2400462.
38 F. Xue, C. Li, Y. Kuang, L. Shi, J. Chen, S. Chen, M. Ma, X. Wang and H. Chen, *Sens. Actuators B: Chem.*, 2022, **369**, 132311.
39 C. Zhao, W. Sun, Y. Zhu, X. Huang, Y. Sun, H.-Y. Wang, Y. Pan and Y. Liu, *J. Med. Chem.*, 2024, **67**, 22322–22331.
40 L. Vachova, V. Novakova, K. Kopecky, M. Miletin and P. Zimcik, *Dalton Trans.*, 2012, **41**, 11651–11656.
41 A. Pal, M. Karmakar, S. R. Bhatta and A. Thakur, *Coord. Chem. Rev.*, 2021, **448**, 214167.
42 J. S. Kim and D. T. Quang, *Chem. Rev.*, 2007, **107**, 3780–3799.
43 X. Li, S. Zhang, J. Cao, N. Xie, T. Liu, B. Yang, Q. He and Y. Hu, *Chem. Commun.*, 2013, **49**, 8656–8658.
44 W. Liu, S. He, X. Ma, C. Lv, H. Gu, J. Cao, J. Du, W. Sun, J. Fan and X. Peng, *Angew. Chem., Int. Ed.*, 2024, **63**, e202411802.
45 J. Gu, X. Li, Z. Zhou, R. Liao, J. Gao, Y. Tang and Q. Wang, *Chem. Eng. J.*, 2019, **368**, 157–164.
46 F. Xiao, D. Lei, C. Liu, Y. Li, W. Ren, J. Li, D. Li, B. Zu and X. Dou, *Angew. Chem., Int. Ed.*, 2024, **63**, e202400453.
47 F. Xu, H. Li, Q. Yao, H. Ge, J. Fan, W. Sun, J. Wang and X. Peng, *Chem. Sci.*, 2019, **10**, 10586–10594.
48 J. Zhang, Y. Zhang, H. Zhang, W. Zhai, X. Shi and C. Li, *J. Mater. Chem. B*, 2023, **11**, 4102–4110.
49 X. Wei, C. Zhang, S. He, J. Huang, J. Huang, S. S. Liew, Z. Zeng and K. Pu, *Angew. Chem., Int. Ed.*, 2022, **61**, e202202966.
50 H. Zhang, C. Shi, F. Han, L. Cai, H. Ma, S. Long, W. Sun, J. Du, J. Fan, X. Chen and X. Peng, *Biomaterials*, 2023, **302**, 122365.
51 J. Huang, J. Liu, J. Wu, M. Xu, Y. Lin and K. Pu, *Angew. Chem., Int. Ed.*, 2024, e202421962.
52 Z. Zhu, Y. Feng, Q. Tian, J. Li, C. Liu, Y. Cheng, S. Zhang, Y. Dang, J. Gao, Y. Lai, F. Zhang, H. Yu, W. Zhang and Z. Xu, *JACS Au*, 2024, **4**, 4032–4042.
53 X. Zhang, Z. Xi, D. Zhang, L. Xu, Y. Xue, X.-D. Jiang and G. Qin, *Chin. Chem. Lett.*, 2025, 111041.
54 S. Guo, D. Gu, Y. Yang, J. Tian and X. Chen, *J. Nanobiotechnol.*, 2023, **21**, 348.
55 J. Luo, Z. Xie, J. W. Y. Lam, L. Cheng, H. Chen, C. Qiu, H. S. Kwok, X. Zhan, Y. Liu, D. Zhu and B. Z. Tang, *Chem. Commun.*, 2001, 1740–1741.
56 J. Mei, N. L. C. Leung, R. T. K. Kwok, J. W. Y. Lam and B. Z. Tang, *Chem. Rev.*, 2015, **115**, 11718–11940.
57 C. Chen, H. Ou, R. Liu and D. Ding, *Adv. Mater.*, 2020, **32**, 1806331.
58 M. Jiang, X. Gu, J. W. Lam, Y. Zhang, R. T. Kwok, K. S. Wong and B. Z. Tang, *Chem. Sci.*, 2017, **8**, 5440–5446.
59 W. Zhang, Y. Chris, R. T. Kwok, J. W. Lam and B. Z. Tang, *J. Mater. Chem. B*, 2018, **6**, 1501–1507.
60 X. Shi, Y. Chris, H. Su, R. T. Kwok, M. Jiang, Z. He, J. W. Lam and B. Z. Tang, *Chem. Sci.*, 2017, **8**, 7014–7024.
61 G. Xu, Y. Tang, Y. Ma, A. Xu and W. Lin, *Spectrochim. Acta - A: Mol. Biomol. Spectrosc.*, 2018, **188**, 197–201.
62 J. Wang, R. Li, H. Ouyang, Y. Lu, H. Fei and Y. Zhao, *Talanta*, 2024, **276**, 126277.
63 Y.-T. Bao, H.-B. Mao, K.-W. Lei, J.-B. Hu and J. Huang, *Talanta*, 2025, **285**, 127392.
64 D. Wang, H. Su, R. T. K. Kwok, X. Hu, H. Zou, Q. Luo, M. M. S. Lee, W. Xu, J. W. Y. Lam and B. Z. Tang, *Chem. Sci.*, 2018, **9**, 3685–3693.
65 Y. Wang, X. Pan, T. Dai, L. Wang, H. Shi, H. Wang and Z. Chen, *Biomater. Sci.*, 2022, **10**, 4866–4875.
66 J. Shi, Z. Wang, C. Shen, T. Pan, L. Xie, M. Xie, L. Huang, Y. Jiang, J. Zhou and W. Zuo, *Dyes Pigm.*, 2022, **200**, 110122.